Supplementary Materials and Methods

2.1 Reagents

Lycopene (502-65-8) was purchased from MedChemExpress (NJ, USA) and its purity was 99.11%. The chemical structure was determined using HPLC and is shown in Supplementary file 1. Curcumin (458-37-7) was purchased from MedChemExpress (NJ, CA, USA), and its purity was 98.16%. A stock solution (5.0 mM) of lycopene was prepared with THF. Different concentrations of working solutions were prepared by diluting the stock solution of lycopene in DMEM or DMEM/F-12K medium or in saline solution. The chemical structure was determined using HPLC and is shown in Supplementary file 2. Oxalic acid (75688) was obtained from Sigma-Aldrich (St. Louis, MO, USA). Antibodies against GSDMD (AF4012, 1:1000 dilution), NLRP3 (DF7438, 1:1000 dilution), IL-1β (AF5103, 1:1000 dilution) and OPN (AF0227, 1:1000 dilution) were purchased from Affinity Biosciences (Melbourne, Australia). The antibody against caspase1 (GB11383, 1:1000 dilution) was purchased from ServiceBio (Wuhan, China). Antibody against IL-6 (ab9324, 1:1000 dilution), α-SMA (ab124964, 1:10000 dilution), and NLRP3 (ab263899, 1:1000) were purchased from Abcam (Cambridge, MA, USA). Antibody against Trappc4 (sc-390551, 1:100 dilution) and IL-1β (sc-12742, 1:200 dilution) were purchased from Santa Cruz Biotechnology (Dallas, Texas, USA). Antibodies against cleaved caspase 3 (9661, 1:1000 dilution), cleaved-caspase1 (4199, 1:1000 dilution), GSDMD (39754, 1:1000 dilution), ERK1/2 (9926, 1:1000 dilution) and p-ERK1/2 (4377, 1:1000 dilution) were purchased from Cell Signaling Technology (Danvers, MA, USA). Vimentin (10366-1-AP, 1:2000 dilution) were purchased from Proteintech (Wuhan, China). An antibody against AMPK (db12601, 1:1000 dilution), PDPK1 (db11455, 1:1000 dilution), and Nup107 (db12683, 1:1000 dilution) were purchased from Diagbio (Hangzhou, China). An antibody against p-AMPK (CY5608, 1:1000 dilution) was purchased from Abways (Shanghai, China). CC90003 (1621999-82-3) and AICAR (681006-28-0) were purchased from TargetMol (Shanghai, China).

2.2 Histology and morphometric analysis

Sections (4 μm thick) were sliced for hematoxylin and eosin (H&E) and von Kossa staining to detect histopathological changes and crystal formation. Crystal deposition was scored as follows: 0, no deposits; 1, papillary tip; 2, cortical-medullary junction; and 3, cortex. If crystals were

discovered in multiple areas, the scores were superimposed for evaluation[1]. Tubular injury was scored according to the percentage of necrotic tubules and the presence of tubular casts from the renal cortices and outer medulla [2]. Apoptotic renal tissues were detected using TUNEL (BrightRed) staining according to the manufacturer's instructions (Servicebio, Wuhan, China). Renal interstitial fibrosis were measured by Masson's trichrome staining according to the manufacturer's instructions (Servicebio, Wuhan, China). Immunohistochemical staining was performed for cleaved-caspase 3, IL-6, OPN, GSDMD, and IL-1β. Immunofluorescent staining for Trappc4 was performed. All results were observed under a bright-light or fluorescence microscope and quantified using the Image J software. Student's t-test was performed to analyze the experimental data between two groups.

2.3 Measurement of 24h urinary and serum variables

Urinary oxalate levels were measured using an oxalate assay kit, according to the manufacturer's instructions (Abcam, Cambridge, MA, USA). The urinary volume and pH were measured manually. Urinary calcium, urea nitrogen and serum creatinine levels were measured using a Beckman Coulter AU5800 automatic biochemical analyzer. Student's t-test was performed to analyze the experimental data between two groups.

2.4 Measurement of oxidative stress indices

The kidney samples were collected and homogenized in PBS using an ultrasonic processor. Supernatants were obtained after centrifugation at 12000 rpm for 15 min at 4°C for ELISA5 (Beyotime, Shanghai, China) detection of MDA, CAT, GSH, and SOD levels. Student's t-test was performed to analyze the experimental data between two groups.

2.5 Western blot analysis

According to the methods described previously[2], cell and tissue lysates were obtained using RIPA buffer. Equivalent amounts of proteins were separated on polyacrylamide gels, transferred to PVDF membranes and immunoblotted with the appropriate antibody. The results were visualized using chemiluminescence. Student's t-test was performed to analyze the experimental data between two groups.

2.6 Cell counting Kit-8 (CCK-8) and cellular lactate dehydrogenase (LDH) assay

RTEC viability was measured using CCK-8 assay (Beyotime, Shanghai, China). The RTECs were seeded in 96-well plates and exposed to oxalate and/or lycopene. RTEC viability was

determined by measuring the absorbance at 450 nm (OD_{450}) after RTECs were treated with a CCK-8 solution for 2 h. LDH levels were measured using an LDH cytotoxicity assay kit (Beyotime, Shanghai, China) and used to evaluate RTEC cell membrane integrity, according to manufacturer's instructions. The absorbance at 490 nm (OD_{490}) was measured using a microplate reader. Student's *t*-test was performed to analyze the experimental data between two groups.

2.7 Intracellular ROS detection and TUNEL fluorescence detection assays

ROS assay kit (Solarbio, Beijing, China) was used to detect intracellular ROS levels after RTECs were incubated with DCFH-DA; The RTECs were incubated with a mixed solution of TdT enzyme and TUNEL reaction buffer to measure apoptotic cells using a TUNEL Apoptosis Detection Kit (Solarbio, Beijing, China). Fluorescence microscopy was used to quantitatively evaluate the ROS and apoptosis levels.

2.8 Transfection of small interfering RNA (siRNA)

NRK-52E cells were transfected with si-Trappc4 or non-targeting siRNA (20 nM) (GenePharma Technology, Shanghai, China) using Lipofectamine 2000 (Invitrogen, Carlsbad, CA). The silencing effect on Trappc4 gene expression in NRK-52E cells was identified using western blot analysis. Student's *t*-test was performed to analyze the experimental data between two groups. The si-Trappc4 sequence was as follows: 5'-CUCUCGAGGUGGCGGAGAATT-3'

2.9 Network pharmacology analysis of the therapeutic effect of lycopene on renal injury induced by calcium oxalate

The Pub-Chem database (http://pubchem.ncbi.nlm.nih.gov/), PharmMapper drug target screening database (http://www.lilab-ecust.cn/pharmmapper/), Super-PRED database (https://prediction.charite.de/index.php?site=chemdoodle_search_target), GeneCard database (https://www.genecards.org/), Disgenet database (https://www.disgenet.org/) and OMIM database (https://omim.org/) were used to predict target genes for lycopene in the treatment of nephrolithiasis, and identify possible signaling pathways.

2.10 Enrichment analysis

KEGG was used to systematically analyze gene functions and signaling pathways associated with the target genes. GO analysis was used to analyze cellular components, biological processes and molecular functions. The cut-off value was set at $P<0.05$.

2.11 Liquid chromatography-mass spectrometry/mass spectrometry (LC-MS/MS) detection

and protein enrichment analysis

An Orbitrap Fusion™ Lumos™ Tribrid™ mass spectrometer (Thermo Fisher Scientific, MA, USA) coupled to a Thermo EASY-nLC system was used for LC-MS/MS detection. Chromatography via a 75 μm × 15 cm nanoViper C18 column (Acclaim PepMap RSLC, 2 μm, 100 A) with a mixture of solvent A and solvent B (solvent A: ddH$_2$O, solvent B: 80 % acetonitrile/ddH$_2$O solution; both containing 0.1 % formic acid) was carried out for peptide separation at a flow rate of 300 nL/min. Gradient elution conditions were as follows: 00:00–45:30 min, 8-28 % solvent B; 45:30–52:30 min, 28–35 % solvent B; 52:30–56:00 min, 35–100 % solvent B; 56:00–60:00 min, 100 % solvent B. The instrument was automatically switched between MS and MS2 scans. The parameters of the full scan MS spectra were as follows: m/z, 350–1,500; resolution, 1.2e4; AGC target, 4.0e5 charges; and maximum injection time (IT), 50 ms. The MS2 parameters were as follows: exclusion duration, 25 s; resolution, 3.0 e4; AGC target, 5.0 e4; maximum IT, 54 ms; and normalized collision energy, 30 %. Peptide and protein identification and quantification were analyzed using Protein Discoverer software (PD 2.4) to search the UniProt database, default settings with static modification of cysteine (+57.0215 Da) and variable oxidation of methionine (+15.9949 Da). The normalized abundance of each identified protein was analyzed using two-tailed Student's *t*-test.

2.12 Molecular docking

The Protein Data Bank (PDB, http://www.rcsb.org/), AutoDock Vina (version 1.1.2) and AutoDockTools (version 1.5.6) were used for the molecular docking analysis after identifying lycopene as the ligand.

2.13 Molecular dynamics (MD) simulation analysis

To assess the reliability of the model constructed via molecular docking, conventional MD simulations were performed using Desmond program (2022-4). The OPLS2005 force field was used to parameterize Trappc4 and lycopene, and the TIP3P model was used to solvate the complexes with water molecules. The Trappc4-lycopene complex was placed in a cubic water box and solvated, followed by neutralization of the system charge with sodium ions and 0.15 M chloride. The steepest descent method was used to minimize the system energy for 50,000 steps. Subsequently, 50,000 NVT and NPT steps equilibration were performed by fixing the positions of the heavy atoms. The system pressure and temperature were maintained at 1 bar and 300 K,

respectively, and an unconstrained 100 ns simulation was conducted following the two equilibration phases. The orbit energy and coordinates were recorded every 10 ps. The interaction modes and dynamic trajectory animations were visualized and analyzed using Maestro 2021 after the trajectory simulation.

2.14 Alanine scanning and saturation mutagenesis by simulation

Alanine scanning was performed for the amino acid residues within a 3 Å radius of the Trappc4-lycopene interface using the virtual amino acid mutant module of Discovery Studio™ 2019 software. Key amino acids were determined by calculating the binding free energy changes before and after the alanine mutation. Saturation mutagenesis was performed to further evaluate the importance of these key amino acids in lycopene binding by mutating the amino acid to each of the other 19 amino acids.

2.15 Cellular thermal shift assay (CETSA)

Total protein (2 mg/mL) extracted from NRK-52E cells was divided into 18 equal fractions. Of these, 9 protein fractions were incubated with lycopene (50 μM) at 37 °C for 10 min, and the others were incubated with DMSO to serve as controls. These samples were then incubated at 9 different temperatures (40-80 °C) for 5 min, respectively, and placed on ice for immediate cooling. Supernatants after centrifugation (4°C and 20,000 g for 15 min) were collected for western blot detection.

2.16 Surface plasmon resonance (SPR) analysis

Briefly, a cell on the CM5 sensor chip was activated with a solution containing N-hydroxysuccinimide (50 μM) and 1-ethyl-3-(3-dimethylaminopropyl) carbodiimide (200 μM) for 420 s at 25 °C and a flow rate of 10 μL/min. 50 μL of Trappc4 protein was then mixed with 180 μL of sodium acetate solution (10 mM, pH 5.0) and immobilized on the cell surface at a flow rate of 10 μL/min for 420 s. After repeating the immobilization steps described above once, the cell was blocked with 1 M ethanolamine (10 μL/min for 420 s). As a control, cells were activated and immobilized in PBS. Both cells were equilibrated with PBS and then with different concentrations of lycopene in PBS at a flow rate of 30 μL/min for 150 s. Cells were regenerated with a 10 mM glycine-HCl solution (pH 2.0) for 5 min at a flow rate of 10 μL/min. Data were acquired using BIAcore T200 Control software (version 2.0, GE Healthcare) and exported as figures using Origin 7 software (version 7.0552, Origin Lab). The Langmuir binding model (1:1)

was used for global fitting of the association and dissociation constants using the BIAcore T200 evaluation software.

2.17 Statistical analysis

All results are represented as means ± standard deviation (SD). Data were analyzed using a two-tailed Student's *t*-test for all comparisons using GraphPad Prism version 9.0. Results were considered statistically significant at *P* values < 0.05.

References:

1. S. R. Mulay, J. Desai, S. V. Kumar, J. N. Eberhard, D. Thomasova, S. Romoli, M. Grigorescu, O. P. Kulkarni, B. Popper, V. Vielhauer, G. Zuchtriegel, C. Reichel, J. H. Bräsen, P. Romagnani, R. Bilyy, L. E. Munoz, M. Herrmann, H. Liapis, S. Krautwald, A. Linkermann and H. J. Anders, Cytotoxicity of crystals involves RIPK3-MLKL-mediated necroptosis, *Nat Commun*, 2016, **7**, 10274.
2. X. Gao, Y. Peng, Z. Fang, L. Li, S. Ming, H. Dong, R. Li, Y. Zhu, W. Zhang, B. Zhu, J. Liao, Z. Wang, M. Liu, W. Li, J. Zeng and X. Gao, Inhibition of EZH2 ameliorates hyperoxaluria-induced kidney injury through the JNK/FoxO3a pathway, *Life Sci* 2022, **291**, 120258.

Supplementary Table1 Results of alanine scanning for determining the key amino acids

Mutation	Mutation energy	Effect of Mutation	VDW Term	Electrostatic Term	Entropy Term	Non-polar Term
A:PHE4>ALA	0.55	DESTABILIZING	0.91	0.01	0.11	0
A:TYR22>ALA	0.91	DESTABILIZING	1.75	0	4.00E-02	0
A:SER23>ALA	-0.04	NEUTRAL	-9.00E-02	0	0	0

A:PRO24>ALA	0.12	NEUTRAL	0.19	0.04	0	0
A:ARG25>ALA	1.08	DESTABILIZING	2.1	0.02	3.00E-02	0
A:PRO101>ALA	0.03	NEUTRAL	1.00E-02	0.03	1.00E-02	0
A:ARG102>ALA	0.72	DESTABILIZING	2.02	0.02	-0.37	0
A:LEU103>ALA	0.84	DESTABILIZING	1.49	0.01	0.11	0
A:LEU111>ALA	0.95	DESTABILIZING	1.56	0.01	0.2	0
A:PHE115>ALA	0.69	DESTABILIZING	1.33	0.02	2.00E-02	0
A:LEU118>ALA	0.36	NEUTRAL	1.45	0.02	-0.47	0
A:PHE119>ALA	0.33	NEUTRAL	0.63	0.02	1.00E-02	0
A:ILE121>ALA	0.35	NEUTRAL	0.96	0.02	-0.17	0
A:GLY122>ALA	-0.01	NEUTRAL	0	0	-1.00E-02	0
A:LEU125>ALA	0.26	NEUTRAL	0.68	0.01	-0.11	0
A:ILE134>ALA	0.29	NEUTRAL	0.6	0.02	-3.00E-02	0
A:LEU137>ALA	0.44	NEUTRAL	1.46	0.01	-0.37	0
A:PHE142>ALA	0.93	DESTABILIZING	1.72	0.02	7.00E-02	0
A:LEU144>ALA	0.76	DESTABILIZING	1.39	0.01	8.00E-02	0
A:LEU158>ALA	0.31	NEUTRAL	0.43	0	0.12	0

Supplementary table2 Results of saturation mutagenesis for determining the key amino acids

Mutation	Mutation energy	Effect of Mutation	VDW Term	Electrostatic Term	Entropy Term	Non-polar Term
A:PHE4>ALA	0.55	DESTABILIZING	0.91	0.01	0.11	0
A:PHE4>ARG	-0.25	NEUTRAL	-0.53	0	2.00E-02	0
A:PHE4>ASN	0.16	NEUTRAL	0.13	0.07	7.00E-02	0
A:PHE4>ASP	0.36	NEUTRAL	0.14	0.49	6.00E-02	0
A:PHE4>CYS	0.33	NEUTRAL	0.61	0.01	3.00E-02	0
A:PHE4>GLN	-0.03	NEUTRAL	-0.22	0.06	6.00E-02	0
A:PHE4>GLU	0.41	NEUTRAL	9.00E-02	0.64	5.00E-02	0
A:PHE4>GLY	0.87	DESTABILIZING	1.41	0.02	0.19	0
A:PHE4>HIS	0.05	NEUTRAL	4.00E-02	0.02	2.00E-02	0
A:PHE4>ILE	-0.14	NEUTRAL	-0.35	0	4.00E-02	0
A:PHE4>LEU	-0.16	NEUTRAL	-0.37	0	3.00E-02	0
A:PHE4>LYS	-0.24	NEUTRAL	-0.69	0.15	4.00E-02	0
A:PHE4>MET	-0.05	NEUTRAL	-0.14	0	2.00E-02	0
A:PHE4>PHE	-0.12	NEUTRAL	-0.25	0	0	0
A:PHE4>PRO	0.27	NEUTRAL	0.43	-0.01	7.00E-02	0
A:PHE4>SER	0.62	DESTABILIZING	0.7	0.05	0.31	0
A:PHE4>THR	0.34	NEUTRAL	0.19	0.03	0.29	0
A:PHE4>TRP	-0.29	NEUTRAL	-0.58	-0.01	1.00E-02	0
A:PHE4>TYR	-0.3	NEUTRAL	-0.61	0	0	0
A:PHE4>VAL	0.2	NEUTRAL	0.27	0.01	8.00E-02	0
A:PHE142>ALA	0.93	DESTABILIZING	1.72	0.02	7.00E-02	0
A:PHE142>ARG	-0.08	NEUTRAL	-1	0.28	0.35	0
A:PHE142>ASN	0.38	NEUTRAL	0.6	0.15	1.00E-02	0
A:PHE142>ASP	0.76	DESTABILIZING	1.15	0.36	1.00E-02	0
A:PHE142>CYS	0.78	DESTABILIZING	1.49	0.01	4.00E-02	0
A:PHE142>GLN	0.84	DESTABILIZING	1.2	0.23	0.16	0
A:PHE142>GLU	0.88	DESTABILIZING	0.61	0.81	0.21	0
A:PHE142>GLY	1.1	DESTABILIZING	2.02	0.02	0.1	0
A:PHE142>HIS	0.08	NEUTRAL	0	0.04	7.00E-02	0
A:PHE142>ILE	0.32	NEUTRAL	0.55	0	6.00E-02	0
A:PHE142>LEU	0.31	NEUTRAL	0.6	0	1.00E-02	0
A:PHE142>LYS	0.16	NEUTRAL	-0.98	0.86	0.28	0
A:PHE142>MET	0.35	NEUTRAL	0.33	0.01	0.22	0
A:PHE142>PHE	-0.07	NEUTRAL	-0.15	0	0	0
A:PHE142>PRO	0.67	DESTABILIZING	1.34	0.01	-1.00E-02	0
A:PHE142>SER	0.78	DESTABILIZING	1.32	0.08	0.1	0
A:PHE142>THR	0.79	DESTABILIZING	1.45	0.02	7.00E-02	0
A:PHE142>TRP	-0.36	NEUTRAL	-0.77	0.06	-1.00E-02	0
A:PHE142>TYR	-0.26	NEUTRAL	-0.72	0.13	4.00E-02	0

| A:PHE142>VAL | 0.51 | DESTABILIZING | 0.92 | 0.01 | 5.00E-02 | 0 |

Supplementary figure1

Supplementary Figure 1
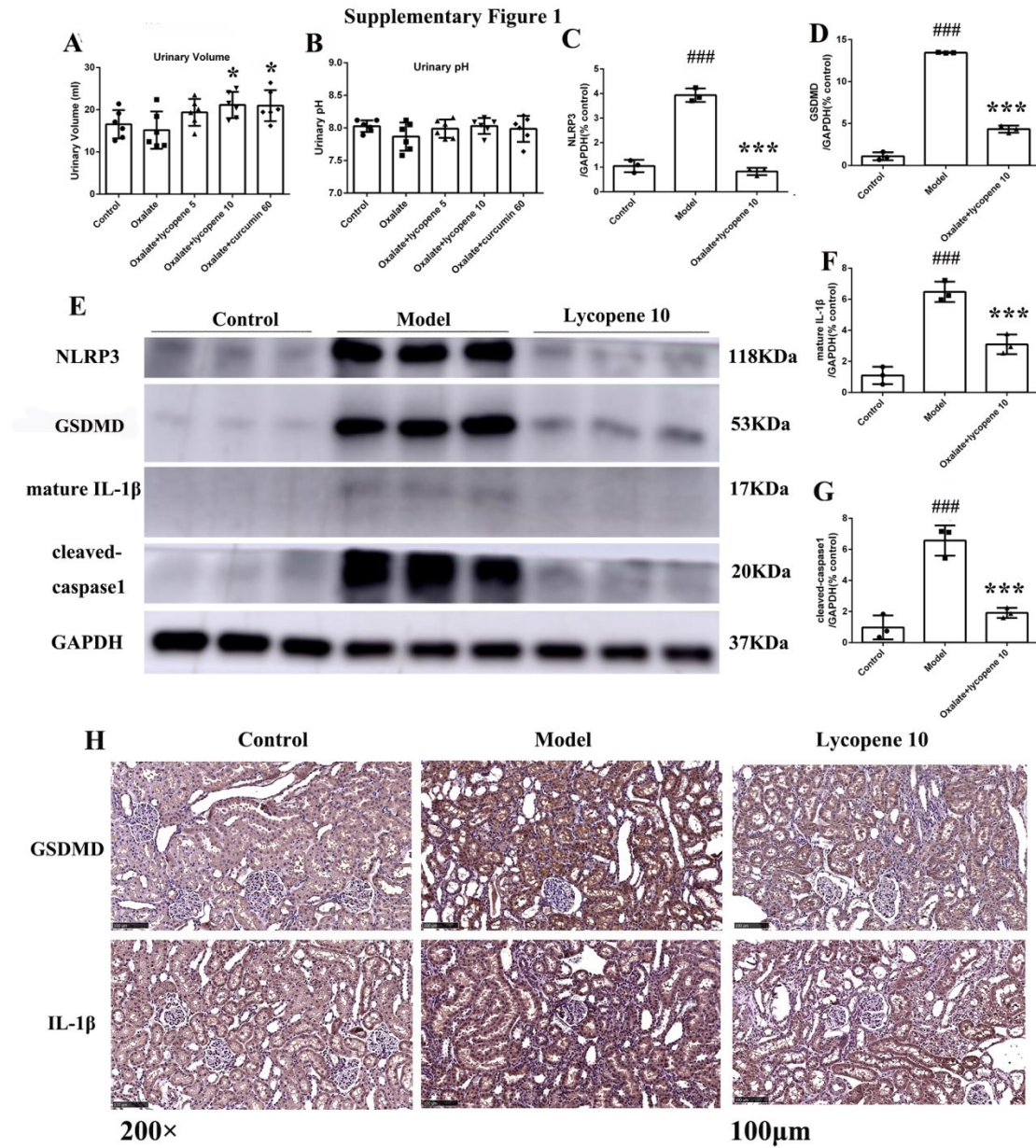
Supplementary figure2

Supplementary Figure 2

A

100μm

B

α-SMA   42KDa

Vimentin   54KDa

GAPDH   37KDa

C   **D**
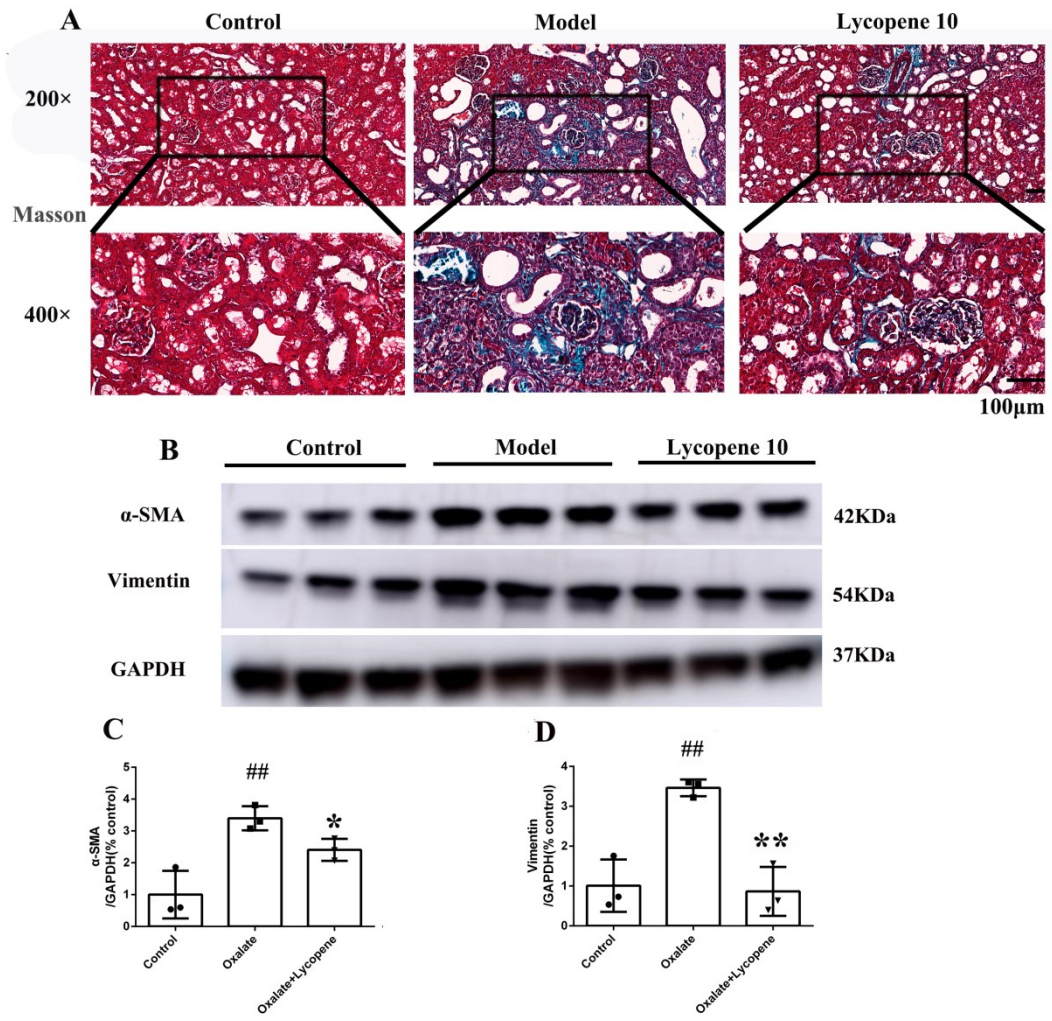
Supplementary figure3

Supplementary Figure 3

NRK-52E

HK-2

G

| | Control | Lycopene 2(μM) | Oxalate | Oxalate+lycopene |

Bright field

TUNEL

ROS

200× 100μm
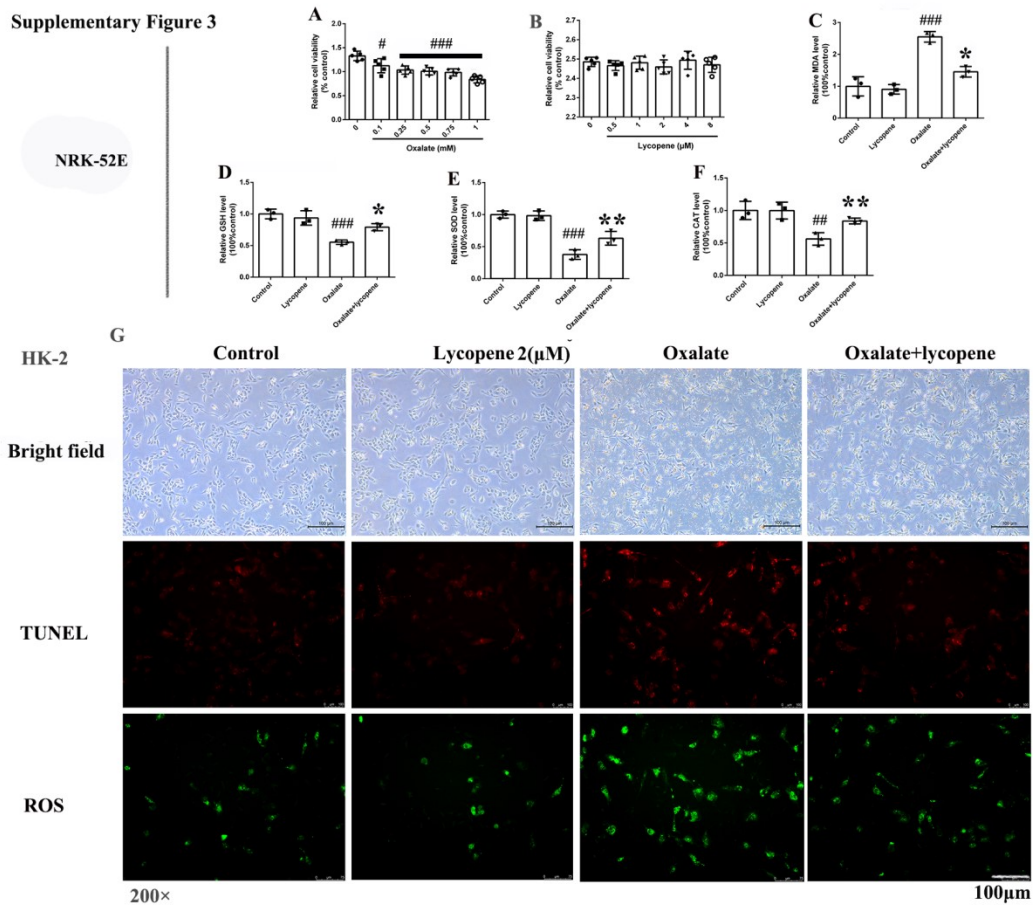
Supplementary figure4

Supplementary Figure4

A

	Control	Oxalate	Oxalate+lycopene 2(μM)	
α-SMA				42KDa
Vimentin				54KDa
GAPDH				37KDa

B

α-SMA

C

Vimentin

Supplementary figure5

A GO analysis from proteomics

B GO analysis from network pharmacology

C

D

E Nup107

F PDPK1

G GAPDH for Nup107 and PDPK1
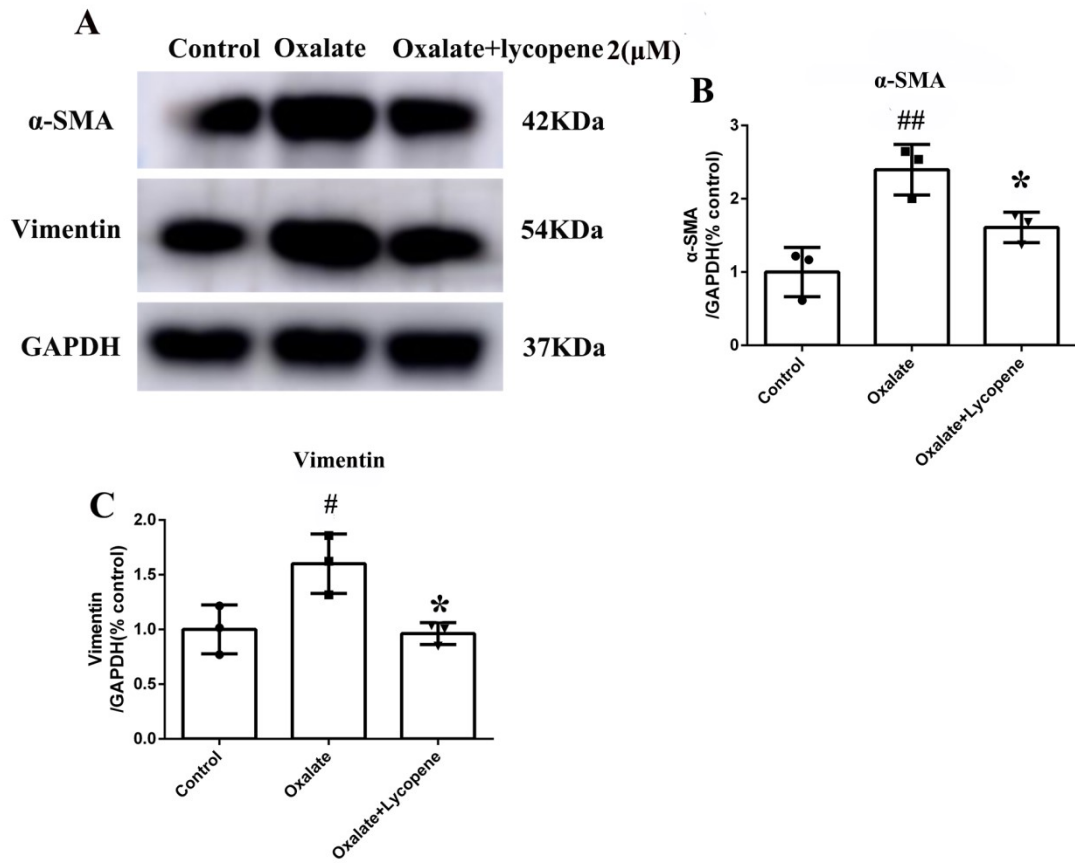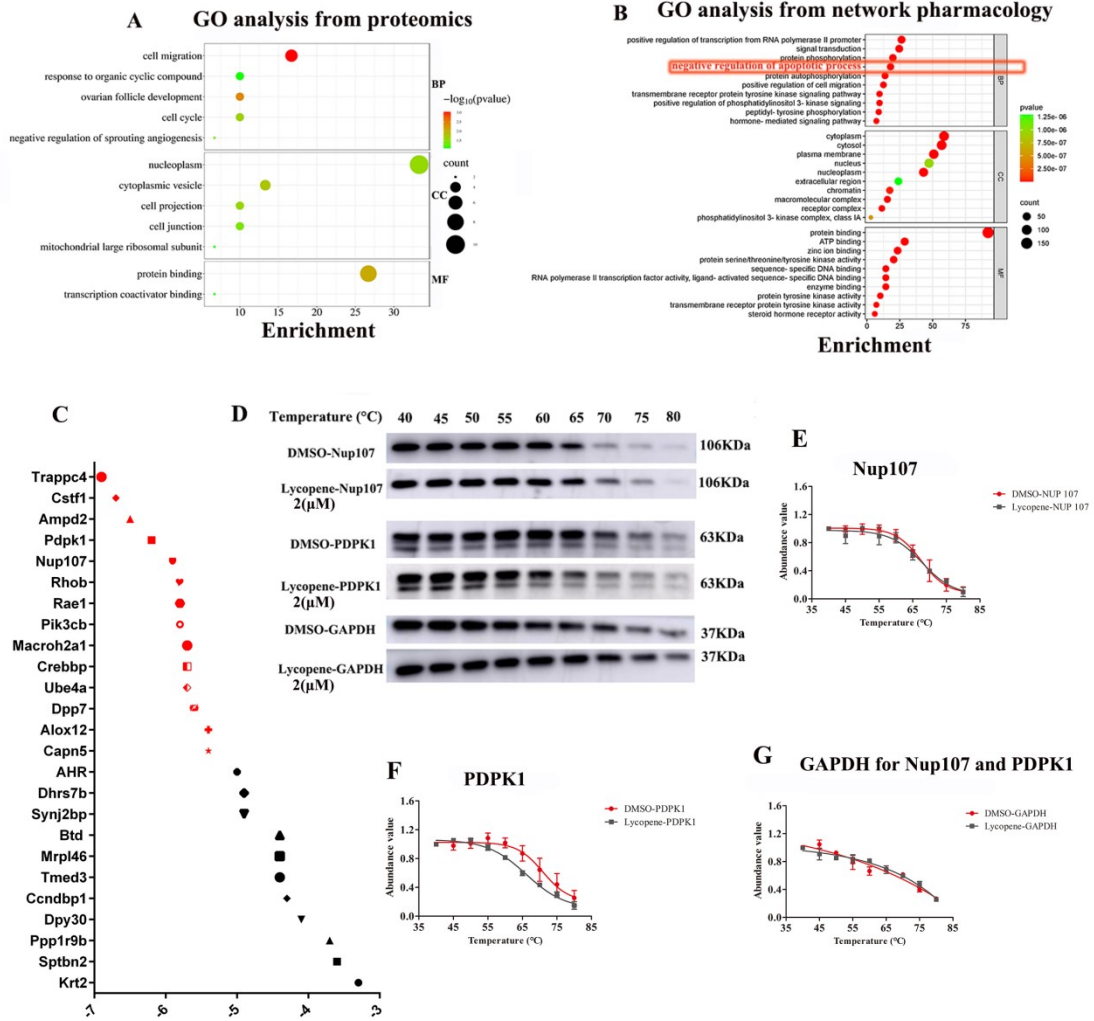
Supplementary figure6

Supplementary Figure 6

A NRK-52E cells

B

C HK-2 cells

D